VSNL1 attenuates hypoxia-induced myocardial apoptosis by regulating the CNP/NPRB pathway

XING YANG[1,2*], WENJUAN FANG[1,3*], RUI CHANG[1], LINLIN MA[1,3], XIAOYAN CHEN[3] and YANFEI LI[1,3]

[1]Department of Scientific Research, Shanghai University of Medicine and Health Sciences Affiliated Zhoupu Hospital, Shanghai 201318, P.R. China; [2]School of Health Science and Engineering, University of Shanghai for Science and Technology, Shanghai 200093, P.R. China; [3]College of Medical Technology, Shanghai University of Medicine and Health Sciences, Shanghai 201318, P.R. China

Received January 10, 2025; Accepted September 19, 2025

DOI: 10.3892/mmr.2026.13863

Abstract. Myocardial apoptosis is a key contributor to the pathogenesis of cardiovascular diseases, driving cardiac dysfunction and disease progression. Visinin-like protein 1 (VSNL1), a protein involved in cardiac pacing and tumor cell apoptosis, may serve a role in myocardial apoptosis. However, its specific function and underlying mechanisms remain unclear. The present study aimed to elucidate the role and molecular pathways of VSNL1 in myocardial apoptosis. Using a hypoxia-induced AC16 cardiomyocyte model, combined with cell transfection, western blotting and biochemical kit detection, a time-dependent decrease in VSNL1 expression was observed under hypoxic conditions. Overexpression of VSNL1 markedly attenuated hypoxia-induced apoptosis, accompanied by a reduction in myocardial injury markers such as malonaldehyde, creatine kinase-MB and lactate dehydrogenase. Furthermore, VSNL1 inhibited excessive reactive oxygen species production and preserved the mitochondrial membrane potential during the early phase of myocardial apoptosis. Conversely, knockdown of VSNL1 exacerbated hypoxia-induced apoptosis, elevated oxidative stress and aggravated mitochondrial dysfunction in cardiomyocytes. Mechanically, VSNL1 was demonstrated to alleviate myocardial apoptosis by upregulating the 2',3'-cyclic nucleotide 3' phosphodiesterase (CNP)/natriuretic peptide receptor B (NPRB) signaling pathway. Notably, the anti-apoptosis effects of VSNL1 were partially reversed by silencing of NPRB, underscoring the critical role of this pathway. Co-immunoprecipitation analysis revealed no direct protein interaction between VSNL1 and CNP, suggesting that VSNL1 regulates the CNP/NPRB pathway through indirect signal transduction rather than physical binding. Furthermore, CNP and NPRB were significantly downregulated at 24 h after permanent ligation of the proximal left anterior descending coronary artery in male C57BL/6 mice and immediately after 24 h of 1% O_2 hypoxia in AC16 cardiomyocytes, indicating early suppression of this protective signaling pathway. Collectively, the findings of the present study suggested that VSNL1 could serve as a potential therapeutic target for hypoxia-induced myocardial apoptosis, providing novel insights into clinical interventions for cardiovascular diseases, particularly in preventing ischemia-related myocardial injury.

Correspondence to: Professor Yanfei Li, Department of Scientific Research, Shanghai University of Medicine and Health Sciences Affiliated Zhoupu Hospital, 1500 Zhou Yuan Road, Pudong New Area, Shanghai 201318, P.R. China
E-mail: liyf@sumhs.edu.cn

Dr Xiaoyan Chen, College of Medical Technology, Shanghai University of Medicine and Health Sciences, 279 Zhouzhu Road, Pudong New Area, Shanghai 201318, P.R. China
E-mail: chenxy@sumhs.edu.cn

*Contributed equally

Key words: apoptosis, hypoxia, visinin-like protein 1, 2',3'-cyclic nucleotide 3' phosphodiesterase/natriuretic peptide receptor B

Introduction

Cardiomyocyte apoptosis serves a pivotal role in the pathogenesis of heart failure (HF) (1), a condition characterized by notable systolic and diastolic dysfunction that compromises the ability of the heart to pump and fill with blood effectively (2). A key contributor to this dysfunction is the reduced oxygen utilization capacity of the failing heart, leading to an inability to meet systemic metabolic demands (3). This metabolic imbalance initiates remodeling processes that exacerbate cardiac dysfunction and accelerate HF progression. Hypoxia-induced cardiomyocyte apoptosis serves a pivotal role in driving HF progression (4).

Excessive reactive oxygen species (ROS) production is a central mechanism underlying hypoxia-induced myocardial injury. Elevated ROS levels cause oxidative damage to cellular components, including lipids, proteins and DNA, thereby impairing membrane integrity and cellular function (5). Under normal physiological conditions, mitochondria are equipped with antioxidant systems to maintain ROS at controlled levels (6). However, hypoxia disrupts mitochondrial function, resulting in a decreased mitochondrial membrane potential (MMP) and the release of cytochrome *c*, further exacerbating mitochondrial damage (7). This mitochondrial dysfunction impairs the respiratory chain, markedly reducing

ATP synthesis, depleting cellular energy and promoting apoptosis (8). These cascading events highlight the critical role of preserving mitochondrial integrity and regulating ROS to maintain cardiomyocyte survival under hypoxic stress.

Visinin-like protein 1 (VSNL1), a member of the neuronal calcium-sensing protein family, is highly expressed in the sinoatrial node, which regulates the pacemaker activity of the heart (9,10). Emerging evidence suggests that VSNL1 serves a crucial role in several biological processes, including cardiac pacing, cell proliferation, tumor progression and neural signaling pathways (10-13). Notably, VSNL1 has been identified as a key anti-apoptotic factor in several cell types, such as colorectal cancer cells, where its downregulation has been reported to induce apoptosis and inhibit cell proliferation (12). Similarly, silencing of VSNL1 in H295R cells has been reported to increase susceptibility to calcium-induced apoptosis (14). However, to the best of our knowledge, the role of VSNL1 in the regulation of myocardial apoptosis remains unexplored and its potential effects in cardiac cells have yet to be determined.

Therefore, the present study established a hypoxia-induced myocardial cell model to assess cardiomyocyte apoptosis, and the changes in ROS levels, the MMP and markers of cellular damage. The expression levels of VSNL1 were modulated to evaluate its role in hypoxia-induced myocardial apoptosis, and the underlying molecular mechanisms were explored. The findings provide novel insights into potential therapeutic targets for myocardial protection and suggest promising clinical strategies for the treatment of cardiovascular diseases.

Materials and methods

Cell treatment. The human AC16 cardiomyocyte cell line (cat. no. MZ-4038; Ningbo Mingzhou Biotechnology Co., Ltd.) was employed in the present study. The cells were cultured in DMEM (Shanghai Basal Media Technologies Co., Ltd.) supplemented with 10% fetal bovine serum (Gibco; Thermo Fisher Scientific, Inc.) and 1% penicillin-streptomycin (Biosharp Life Sciences) at 37˚C in a humidified atmosphere containing 5% CO_2. To induce apoptosis, AC16 cardiomyocytes were subjected to hypoxic conditions in a modular incubator (Thermo Fisher Scientific, Inc.) with a gas mixture of 94% N_2, 5% CO_2 and 1% O_2 for 24 h at 37˚C. The control group was maintained under normoxic conditions with 95% air and 5% CO_2. When time-series data were required, parallel cultures were exposed for 0 h, 10 min, 1, 6 or 24 h.

Lactate dehydrogenase (LDH) release assay. Cells were exposed to hypoxic conditions (94% N_2, 5% CO_2, 1% O_2) at 37˚C for 24 h. Following treatment of cells from each group, the cell culture supernatants were collected. The supernatants were then combined with an LDH assay working solution (cat. no. C0016; Beyotime Institute of Biotechnology) and the resulting mixture was incubated at room temperature in the dark for 30 min. After incubation, the absorbance was measured at 490 nm to determine the LDH activity.

Measurement of creatine kinase-MB (CK-MB) levels. The concentration of CK-MB in the cell supernatants was determined using an ELISA kit (cat. no. H197-1-2; Nanjing Jiancheng Bioengineering Institute) according to the manufacturer's instructions.

ROS level assessment. Cells were seeded in 6-well plates at a density of $5x10^5$ cells/well and cultured at 37˚C in a humidified atmosphere containing 5% CO_2. After overnight incubation, the cells were exposed to hypoxic conditions (94% N_2, 5% CO_2, 1% O_2) at 37˚C for 24 h. After removing the culture medium, 2'-7'-dichlorodihydrofluorescein diacetate (Beyotime Institute of Biotechnology) diluted in serum-free DMEM was added to the cells and cells were incubated for 20 min at 37˚C. Following three washes with serum-free DMEM, ROS levels were observed under a fluorescence microscope (Olympus Corporation) and analyzed using ImageJ software (version 1.53e; National Institutes of Health, USA). Single-cell suspensions were then collected and analyzed using a NovoCyte Penteon flow cytometer (Agilent Technologies, Inc.) with NovoExpress software (version 1.5.0; Agilent Technologies, Inc.) (15).

Measurement of malonaldehyde (MDA) levels. MDA levels were determined using a commercial assay kit (cat. no. S0131; Beyotime Institute of Biotechnology). Briefly, cells were lysed on ice with RIPA buffer (cat. no. P0013C; Beyotime Institute of Biotechnology), and after centrifugation at 11,100 x g for 15 min at 4˚C, the supernatant was collected for subsequent analysis. MDA concentrations in the supernatant were quantified at 532 nm using a microplate reader (PT3502PC; Beijing Potenov Xinqiao Technology Co., Ltd.), according to the manufacturer's protocol. MDA levels were normalized to the protein concentration. Protein concentration was determined using the BCA protein assay kit (cat. no. P0010; Beyotime Institute of Biotechnology) according to the manufacturer's instructions.

VSNL1 lentivirus infection. For lentivirus-induced overexpression of VSNL1, AC16 cells were seeded at a density of $1x10^4$ cells/well in 96-well plates (100 μl/well) and were incubated overnight at 37˚C in a 5% CO_2 incubator. The recombinant lentiviral vector pHBLV-CMV-MCS-3FLAG-EF1-ZsGreen-T2A-PURO (Hanbio Biotechnology Co., Ltd.) was used to generate the virus using a 3rd generation lentiviral packaging system. Lentiviral particles were produced by co-transfecting 293T cells (cat. no. CRL-3216; American Type Culture Collection) with 4 μg VSNL1 plasmid, 3 μg packaging plasmid (pCMV-dR8.91) and 1 μg envelope plasmid (pCMV-VSV-G) (Hanbio Biotechnology Co., Ltd.) at a ratio of 4:3:1 using Lipofectamine® 3000 (Invitrogen; Thermo Fisher Scientific, Inc.). Transfection was performed at 37˚C for 48 h. Viral supernatants were collected at 48 and 72 h post-transfection, filtered through a 0.45-μm membrane, and stored at -80˚C.

For infection, the virus was thawed on ice, diluted in fresh medium and added to AC16 cells at 30-50% confluence at a multiplicity of infection of 10. On day 1 post-infection (~24 h), the virus-containing medium was removed and replaced with fresh complete medium. The cells were incubated at 37˚C for an additional 48 h, and then harvested at 72 h post-infection for further experiments. Stable cell lines were selected with

medium containing 2 μg/ml puromycin (Sigma-Aldrich; Merck KGaA) for 7 days, followed by maintenance in medium with 1 μg/ml puromycin.

Cell transfection. Cell transfection using Lipofectamine 3000 (Invitrogen; Thermo Fisher Scientific, Inc.) resulted in the downregulation of natriuretic peptide receptor B (NPRB) and VSNL1 in AC16 cardiomyocytes. The small interfering RNAs (siRNAs) used in the present study included a sequence targeting human VSNL1 (si-VSNL1; 5'-CGACCCTTCCATTGTATTA-3'), a sequence targeting human NPRB (si-NPRB; 5'-GACGACCCATCCTGTGATA-3') and a non-targeting negative control (cat. no. siN0000001-1-5); all purchased from Guangzhou RiboBio Co., Ltd. The specific sequence of non-targeting negative control was not provided by the supplier. Prior to transfection, the original culture medium was replaced with fresh high-glucose DMEM supplemented with 10% FBS and 1% penicillin-streptomycin. The transfection mixture was prepared by mixing 50 nM siRNA with 5 μl Lipofectamine 3000 in Opti-MEM reduced serum medium (Gibco; Thermo Fisher Scientific, Inc.). To form a lipoplex, the transfection mixture was incubated at room temperature for 15 min. After 15 min, the transfection mixture was added to the cells, and the cells were continuously cultured in a 37˚C incubator with 5% CO_2 without replacing the medium containing the transfection mixture for 6 h. After 6 h of incubation with the transfection mixture, the medium was aspirated and replaced with fresh complete high-glucose DMEM (10% FBS, 1% penicillin-streptomycin), and the cells were further cultured under the same conditions until 48 h post-transfection (i.e., 42 h after medium replacement). The subsequent experiments were performed at this 48 h time point.

Reverse transcription-quantitative PCR (RT-qPCR). Total RNA was isolated from AC16 cells using TRIzol® (Invitrogen; Thermo Fisher Scientific, Inc.) according to the manufacturer's instructions. The RNA concentration was determined using a NanoDrop® spectrophotometer (Thermo Fisher Scientific, Inc.). For complementary DNA synthesis, RNA was incubated at 42˚C for 15 min, followed by a 5-sec heat treatment at 85˚C, as described in the manufacturer's instructions of the TransScript® Green Two-Step qRT-PCR SuperMix kit (Thermo Fisher Scientific, Inc.). The primer sequences used for human AC16 cells were as follows: VSNL1 forward, 5'-TATGACCTGGATGGTGATGGCAAG-3' and reverse, 5'-AATCTTGTCTACTCGCTGCTCAGG-3'; 2',3'-cyclic nucleotide 3' phosphodiesterase (CNP) forward, 5'-ATGGTGT CGGCTGACGCTTAC-3' and reverse, 5'-CGTTCGTGGTTG GTGTCATCAAG-3'; NPRB forward, 5'-CTGCGCATGGAA CAGTATGC-3' and reverse, 5'-GGGTGCTCTCTGCTGACA AT-3'; BAX forward, 5'-CCCCCGAGAGGTCTTTTTCC-3' and reverse, 5'-TGTCCAGCCCATGATGGTTC-3'; BCL-2 forward, 5'-GGGATTCCTGCGGATTGACA-3' and reverse, 5'-TGCATAAGGCAACGATCCCA-3'; and β-actin forward, 5'-GGGAAATCGTGCGTGACATTAAG-3' and reverse, 5'-TGTGTTGGCGTACAGGTCTTTG-3'. Each primer mix was loaded into a 96-well fluorescent RT-PCR plate, and RT-PCR was performed using the CFX Connect system (Bio-Rad Laboratories, Inc.). The thermocycling parameters were as follows: Initial denaturation step at 94˚C for 30 sec, followed by 40 cycles of 5 sec at 94˚C and 30 sec at 60˚C. mRNA expression levels were determined using the $2^{-\Delta\Delta Cq}$ method (16). All experiments were independently replicated three times.

Western blot analysis. Total proteins were extracted from both AC16 cardiomyocytes and mouse cardiac tissues using RIPA lysis buffer containing protease and phosphatase inhibitors (cat. no. P0039; Beyotime Institute of Biotechnology). For myocardial tissue samples, freshly collected heart tissue was weighed and immediately homogenized in ice-cold RIPA buffer using a mechanical homogenizer. Following homogenization, the samples were incubated on ice for 30 min and then centrifuged at 11,100 x g for 15 min at 4˚C. For cell samples, cultured cells were washed twice with PBS, lysed directly in RIPA buffer and centrifuged under the same conditions. The supernatants containing total proteins were collected, and protein concentrations were determined using a BCA protein assay kit (Thermo Fisher Scientific, Inc.). Equal amounts of protein (30 μg) were separated by SDS-PAGE on 10% gels and transferred onto PVDF membranes. The membranes were blocked in 5% milk at room temperature for 1 h, and incubated overnight at 4˚C with primary antibodies. The antibodies used were as follows: VSNL1 (1:400; cat. no. A2797; ABclonal Biotech Co., Ltd.), NPRB (1:1,000; cat. no. 55113-1-AP; Proteintech Group, Inc.), CNP (1:1,000; cat. no. 13427-1-AP; Proteintech Group, Inc.), BCL-2 (1:1,000; cat. no. 26593-1-AP; Proteintech Group, Inc.), BAX (1:1,000; cat. no. 50599-2-IG; Proteintech Group, Inc.) and β-actin (1:10,000; cat. no. 66009-1-IG; Proteintech Group, Inc.). Subsequently, the membranes were incubated with HRP-conjugated secondary antibodies, including anti-rabbit (1:5,000; cat. no. SA00001-2; Proteintech Group, Inc.) and anti-mouse secondary antibodies (1:5,000; cat. no. SA00001-1; Proteintech Group, Inc.) for 1 h at room temperature. After antibody binding, chemiluminescent detection was performed using BeyoECL Moon (cat. no. P0018FS; Beyotime Institute of Biotechnology) and band visualization was performed on the Tanon 4600 Chemiluminescence Imaging System (Tanon Science and Technology Co., Ltd.).

Analysis of the VSNL1 expression profile. To assess the expression profile of VSNL1 across various normal human tissues, data were retrieved from the Human Protein Atlas (HPA) database (https://www.proteinatlas.org). This freely accessible online resource offers extensive information on human protein expression in numerous normal tissues and cell lines. Relevant data on VSNL1 expression were obtained to analyze its tissue-specific distribution and expression pattern.

MMP assessment. The MMP was evaluated using the Enhanced MMP Assay Kit with JC-1 (Beyotime Institute of Biotechnology). After removing the culture medium, cells in 6-well plates were incubated with a mixture of 1 ml cell culture medium and 1 ml JC-1 staining solution for 20 min at 37˚C. Following incubation, cells were washed twice with JC-1 staining buffer and then visualized under a fluorescence microscope (Olympus Corporation). Image analysis was performed using ImageJ software (version 1.8.0_172; National Institutes of Health).

Intracellular calcium measurement. Intracellular Ca^{2+} levels were measured using the Calcium Assay Kit (cat. no. S1063S; Beyotime Institute of Biotechnology) according to the manufacturer's instructions. Briefly, AC16 cells were lysed and centrifuged at 12,000 x g for 30 min at 4˚C to collect supernatants. Standards and samples were added to a 96-well plate, followed by the assay working solution. After incubation at room temperature for 5-10 min in the dark, absorbance was measured at 575 nm. Calcium concentrations were calculated from a standard curve.

Co-immunoprecipitation (Co-IP) experiment. To assess whether there is a protein-protein interaction between VSNL1 and CNP, Co-IP technology was applied in AC16 cells in the present study. Initially, AC16 cells grown to 80-90% confluence in 10-cm dishes were treated with 500 μl lysis buffer per dish. The lysis buffer contained 1% NP-40, 150 mM NaCl, 50 mM Tris-HCl (pH 7.5) and protease inhibitors (1 mM PMSF and 1 μg/ml aprotinin; cat. no. P1049; Beyotime Institute of Biotechnology). The cells were then incubated on ice for 30 min. The lysate was then centrifuged at 12,000 x g for 15 min at 4˚C, and the supernatant was collected for further analysis. For each IP reaction, 500 μg total protein (equivalent to 200 μl supernatant) was incubated overnight at 4˚C with either specific primary antibodies against VSNL1 (2 μg; cat. no. A2797; ABclonal Biotech Co., Ltd.) or CNP (2 μg; cat. no. 13427-1-AP; Proteintech Group, Inc.), or with isotype control IgG antibodies (2 μg; cat. no. AC005; ABclonal Biotech Co., Ltd.) as a negative control. To capture antibody-protein immunocomplexes, 50 μl 50% (v/v) Protein A/G agarose bead slurry (equivalent to 25 μl packed agarose beads; cat. no. 20421; Thermo Fisher Scientific, Inc.) was added to each IP reaction mixture, which was then gently rotated at 4˚C for 4-6 h to allow sufficient bead-antibody-antigen complex formation. The immunoprecipitates were washed five times with ice-cold wash buffer (same formulation as the lysis buffer without the protease inhibitors) to remove nonspecific binding proteins. Immunocomplexes were isolated by centrifugation at 3000 x g for 5 min at 4˚C to pellet the beads, followed by aspiration of the supernatant. The pellets were resuspended in 30 μl 2X SDS sample buffer and boiled at 95˚C for 10 min to elute the proteins from the beads. The eluted products were separated by SDS-PAGE on 10% gels, transferred onto a PVDF membrane and analyzed by western blotting, as aforementioned, to assess the co-precipitation of CNP and VSNL1. Co-precipitation of CNP with VSNL1 would suggest a potential protein-protein interaction between the two.

Establishment of acute myocardial infarction (AMI) model. A total of 30 male C57BL/6 mice (age, 8-10 weeks; weight, 22-25 g) were purchased from Beijing Vital River Laboratory Animal Technology Co., Ltd.; Charles River Laboratories, and were used in the present study. Mice were housed in a specific pathogen-free facility under the following controlled conditions: Temperature 22±2˚C, relative humidity 50±10% and a 12-h light/dark cycle (lights on at 7:00 a.m. and off at 7:00 p.m.). Animals had free access to standard laboratory chow and sterile water throughout the experimental period.

Mice were randomly assigned to two experimental groups: An AMI group or a sham-operated control group. The AMI group underwent left anterior descending (LAD) coronary artery ligation at the proximal one-third segment to induce ischemia, while the sham group received the same surgical procedure without ligation. All procedures were performed under general anesthesia using isoflurane (3% for induction and 1.5-2% for maintenance). AMI was induced by permanent ligation of the LAD coronary artery with a 6-0 silk suture. In the sham-operated group, the LAD coronary artery was passed with the suture needle but not ligated, serving as a surgical control.

All animal protocols were approved by the Ethics Committee of Shanghai University of Medicine and Health Sciences (Shanghai, China; approval no. 2021-SZR-05-410482198512239314) and the present study conformed to institutional and national guidelines for the care and use of laboratory animals.

For sacrifice, mice were confirmed to be under deep anesthesia with isoflurane, followed by the intraperitoneal injection of 150 mg/kg pentobarbital sodium. Mortality was verified by the absence of heartbeat, respiration and reflex responses.

Echocardiographic assessment. Transthoracic echocardiography was performed 24 h after the establishment of the AMI model using the Vevo 2100 high-resolution imaging system (FUJIFILM VisualSonics, Inc.) equipped with a 30-MHz transducer. Mice were anesthetized with 3% isoflurane for induction and 1.5% isoflurane for maintenance and then positioned supine on a temperature-controlled platform. After hair removal in the precordial region, a pre-warmed ultrasound gel was applied to ensure optimal acoustic coupling. M-mode images were captured from the parasternal long-axis view at the level of the papillary muscles to evaluate cardiac function.

Assessment of myocardial infarct size using 2,3,5-triphenyltetrazolium chloride (TTC) staining. To evaluate infarct size, hearts were harvested immediately after euthanasia. The isolated hearts were first rinsed in cold saline and then incubated in 1% TTC solution prepared in Tris buffer at 37˚C for 15 min.

Statistical analysis. Statistical analysis was performed using GraphPad Prism 8.0 software (Dotmatics). Data are presented as the mean ± standard deviation from at least three independent experiments. Two-tailed unpaired Student's t-test was used for two-group comparisons; one-way ANOVA followed by Tukey's post hoc test was used for multiple-group comparisons. $P<0.05$ was considered to indicate a statistically significant difference.

Results

Hypoxia induces apoptosis in cardiomyocytes. To assess the effects of hypoxia on apoptosis and cellular damage, a hypoxia-induced cardiomyocyte model was established. AC16 cardiomyocytes, exposed to hypoxia for 24 h, exhibited significant downregulation of BCL-2 mRNA expression and upregulation of BAX mRNA expression. The results indicated that prolonged hypoxia activated apoptotic pathways (Fig. 1A and B).

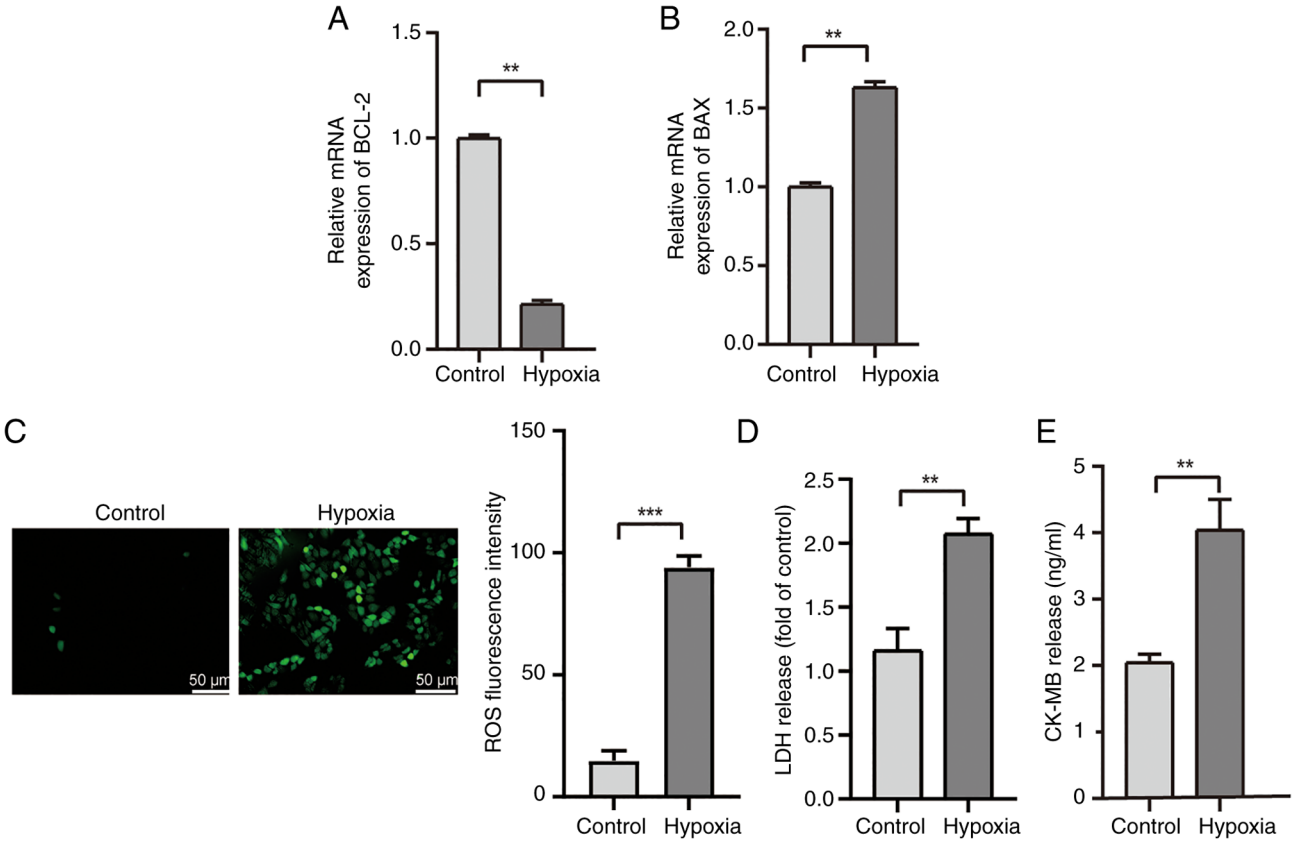

Figure 1. Hypoxia-induced apoptosis in cardiomyocytes. Relative mRNA expression levels of apoptotic genes (A) BCL-2 and (B) BAX in AC16 cardiomyocytes cultured under control or hypoxic conditions for 24 h. (C) ROS levels were measured using biochemical kits. Scale bar, 50 μm. (D) LDH release assay to quantify LDH levels following hypoxic treatment. (E) ELISA detection of CK-MB levels in AC16 cardiomyocytes subjected to hypoxia. **P<0.01, ***P<0.001. ROS, reactive oxygen species; LDH, lactate dehydrogenase; CK-MB, creatine kinase-MB.

As excessive production of ROS can trigger oxidative stress, damage proteins, lipids and DNA in cells, and further activate apoptosis signaling pathways (17), the present study analyzed intracellular ROS levels and the release of myocardial injury markers LDH and CK-MB (Fig. 1C-E). Hypoxia exposure resulted in a substantial increase in ROS levels, accompanied by pronounced elevations in LDH and CK-MB release, signifying severe oxidative stress and cellular injury.

Collectively, these findings indicated that hypoxia may induce oxidative stress and subsequent apoptosis. This established a robust experimental model for further mechanistic studies on the role of VSNL1 in cardiomyocyte apoptosis under hypoxic conditions.

Hypoxia induces downregulation of VSNL1 expression in cardiomyocytes. To evaluate the expression profile of VSNL1 in several normal human tissues, data from the HPA database (https://www.proteinatlas.org) were analyzed (Fig. 2A). The results revealed that VSNL1 expression was markedly higher in cardiomyocytes compared with in other tissues. Subsequently, AC16 cells were exposed to hypoxic conditions for 0 min, 10 min, 1 h, 6 h and 24 h, and the mRNA and protein expression levels of VSNL1 were assessed using qPCR and western blotting, respectively. The results revealed a significant reduction in VSNL1 expression after 24 h of hypoxia (Fig. 2B and C).

These findings suggested that hypoxia markedly downregulated VSNL1 expression in cardiomyocytes, potentially indicating its involvement in the pathophysiology of hypoxia-induced cardiac injury.

Establishment and validation of the AMI mouse model. To further assess whether the aforementioned regulation also occurs *in vivo*, an AMI model was established in mice via permanent ligation of the LAD coronary artery. Mice were randomly assigned to an AMI group or a sham-operated control group. Successful induction of infarction was confirmed by TTC staining, which showed pale infarcted regions in AMI mice and red-stained viable myocardium in sham controls (Fig. 3A). Echocardiographic assessment revealed significant reductions in the left ventricular ejection fraction and fractional shortening in AMI mice compared with the sham group (Fig. 3B-D), indicating impaired cardiac function. Consistent with the *in vitro* findings, western blot analysis demonstrated that VSNL1 expression was markedly decreased in the myocardial tissue of AMI mice (Fig. 3E), supporting its potential role in the pathogenesis of ischemic heart injury.

VSNL1 inhibits cardiomyocyte apoptosis under hypoxic conditions. Subsequently, the role of VSNL1 in regulating hypoxia-induced cardiomyocyte apoptosis was assessed using VSNL1 overexpression and silencing. qPCR and western blot analyses demonstrated that lentivirus-mediated VSNL1 overexpression markedly increased VSNL1 RNA and protein

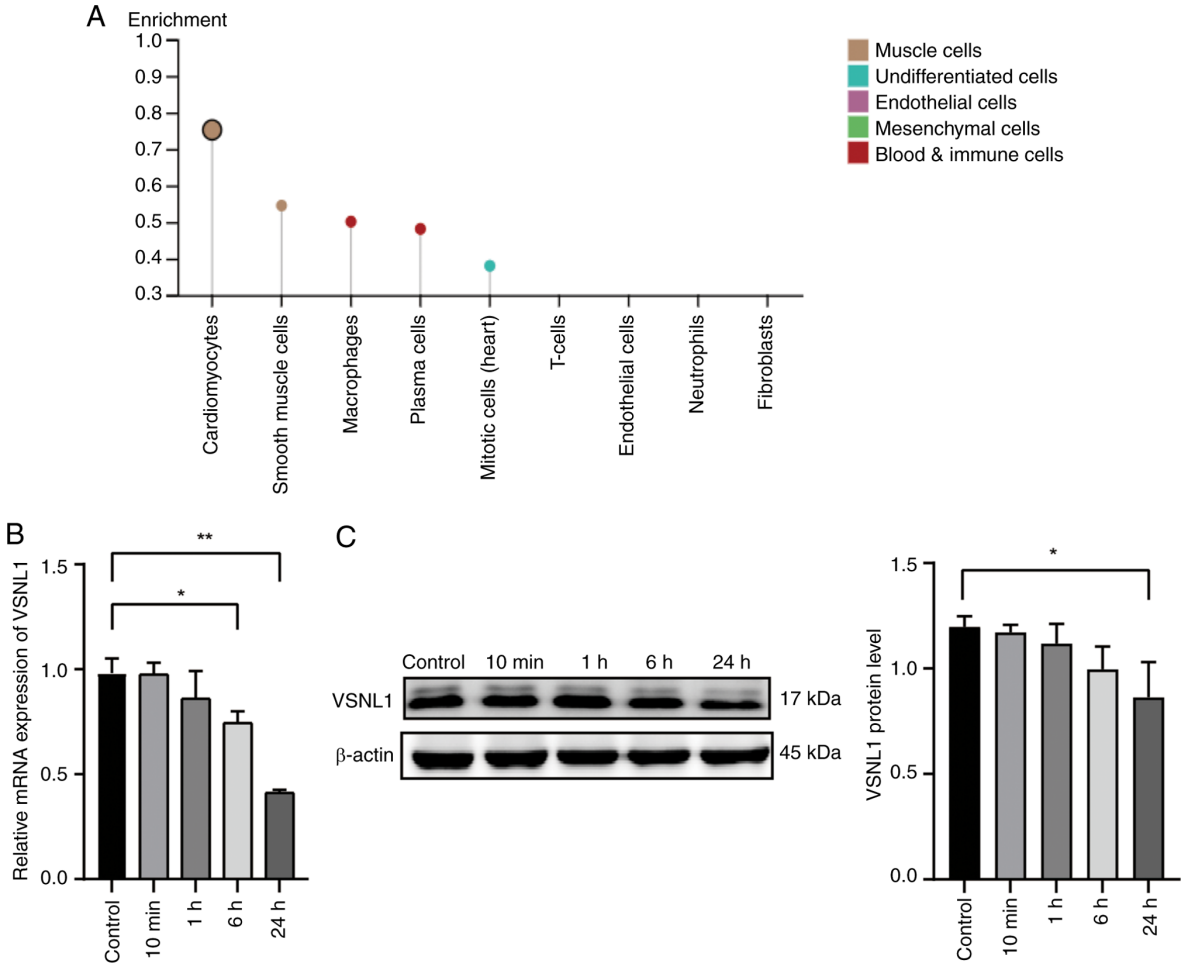

Figure 2. Hypoxia-induced downregulation of VSNL1 expression in cardiomyocytes. (A) Analysis of VSNL1 expression in human tissues was conducted using the public Human Protein Atlas database. (B) Changes in VSNL1 mRNA levels in AC16 cells at different times of hypoxia injury. (C) Changes in VSNL1 protein levels in AC16 cells at different times of hypoxia injury, and semi-quantification of the VSNL1 protein level. *P<0.05, **P<0.01. VSNL1, visinin-like protein 1.

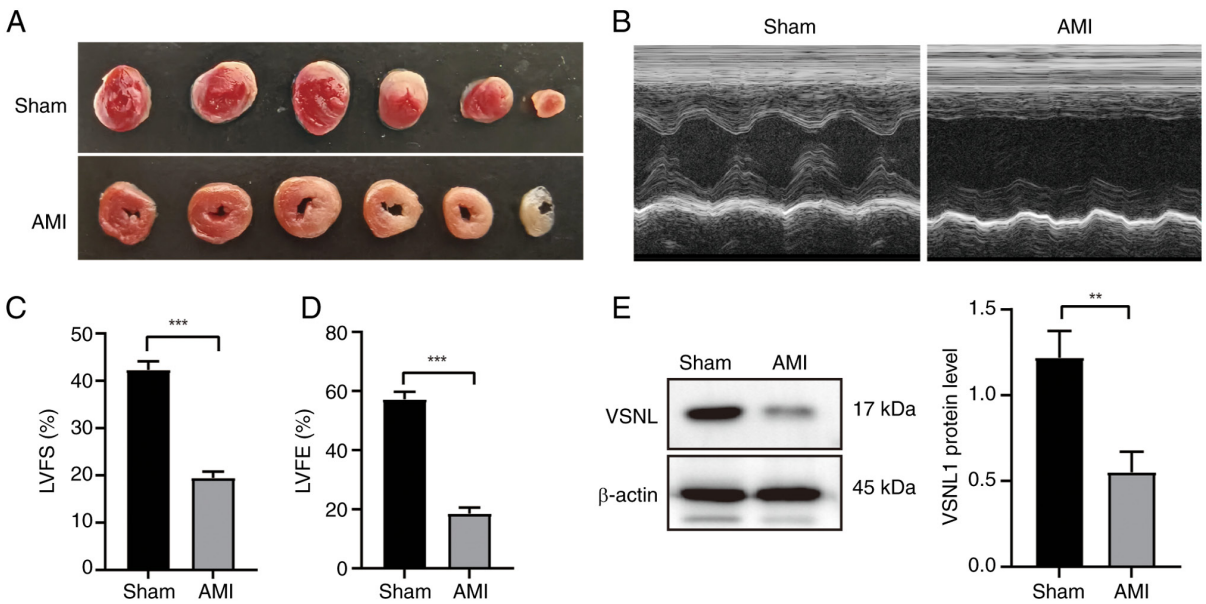

Figure 3. Validation of the AMI mouse model and downregulation of VSNL1 expression. (A) Representative 2,3,5-triphenyltetrazolium chloride staining of heart sections from Sham and AMI groups, showing viable myocardium in red and infarcted areas in pale color. (B) M-mode echocardiography images at 24 h post-surgery. Quantitative comparison of (C) LVFS and (D) LVEF between Sham and AMI groups, demonstrating significant impairment of cardiac function in the AMI group. (E) Western blot analysis showing reduced protein expression levels of VSNL1 in myocardial tissue from AMI mice. **P<0.01, ***P<0.001. AMI, acute myocardial infarction; VSNL1, visinin-like protein 1; LVFS, left ventricular fractional shortening; LVEF, left ventricular ejection fraction.

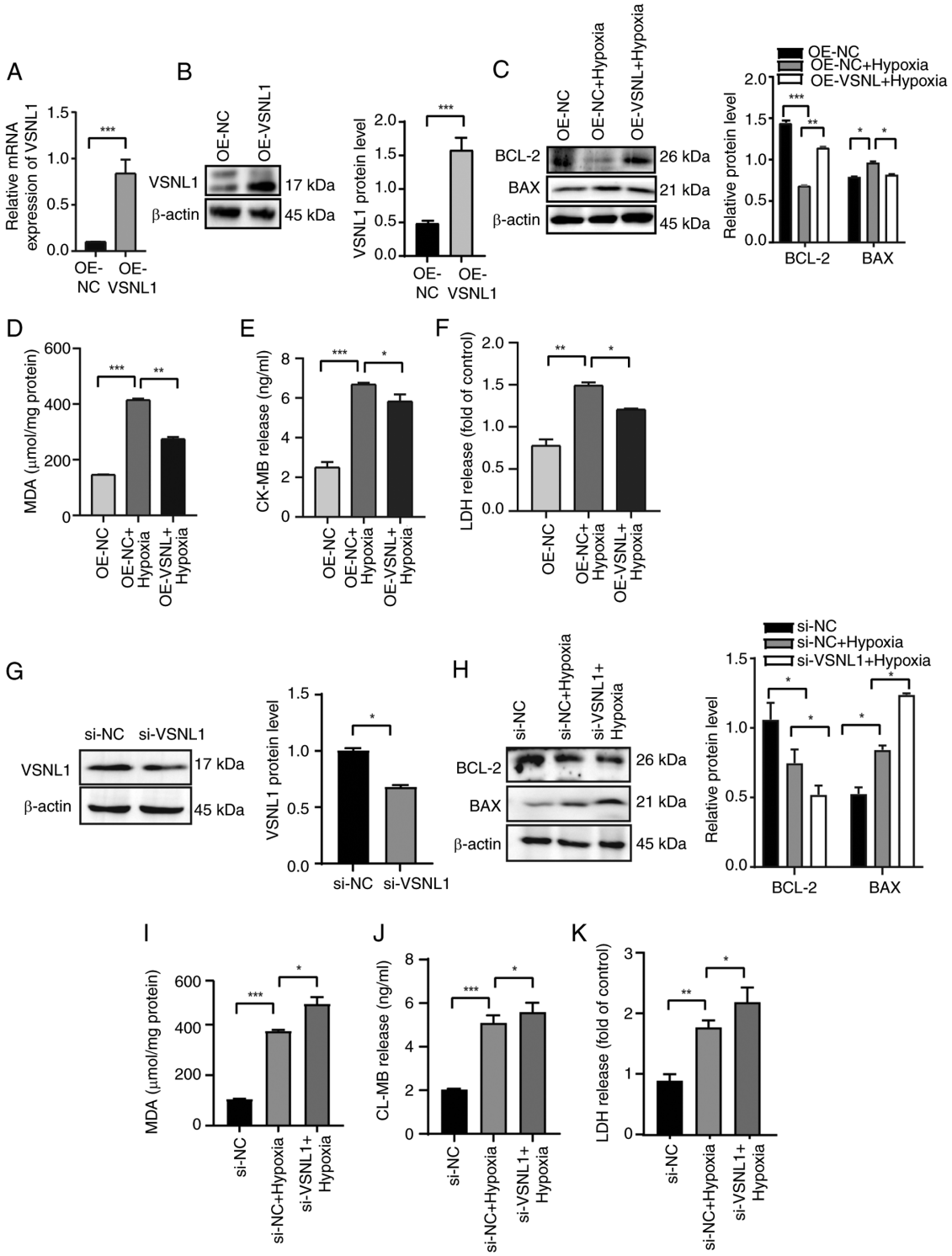

Figure 4. Regulatory role of VSNL1 in hypoxia-induced cardiomyocyte apoptosis. (A and B) AC16 cardiomyocytes were infected with a lentivirus overexpressing VSNL1. VSNL1 expression was assessed by (A) quantitative PCR and (B) western blotting. (C) Western blot analysis of BCL-2 and BAX protein expression in AC16 cells following VSNL1 overexpression, along with semi-quantification of BCL-2 and BAX protein levels. The levels of (D) MDA, (E) CK-MB and (F) LDH were measured using specific assay kits after VSNL1 overexpression. (G) VSNL1 expression in AC16 cells post-transfection with siRNA was assessed by western blotting. (H) Western blot analysis of BCL-2 and BAX protein expression following VSNL1 silencing, with semi-quantification of BCL-2 and BAX protein levels. The levels of (I) MDA, (J) CK-MB and (K) LDH were measured using specific assay kits following VSNL1 silencing. *P<0.05, **P<0.01, ***P<0.001. VSNL1, visinin-like protein 1; OE-NC, overexpression negative control; OE-VSNL1, VSNL1 overexpression; siRNA, small interfering RNA; si-NC, siRNA negative control; si-VSNL1, VSNL1 knockdown via siRNA; MDA, malonaldehyde; CK-MB, creatine kinase-MB; LDH, lactate dehydrogenase.

levels in AC16 cells (Fig. 4A and B), whilst siRNA-mediated silencing of VSNL1 markedly reduced VSNL1 protein expression (Fig. 4G). Following hypoxia treatment, VSNL1 overexpression markedly upregulated the anti-apoptotic protein BCL-2 and downregulated the pro-apoptotic protein BAX (Fig. 4C). By contrast, VSNL1 silencing decreased

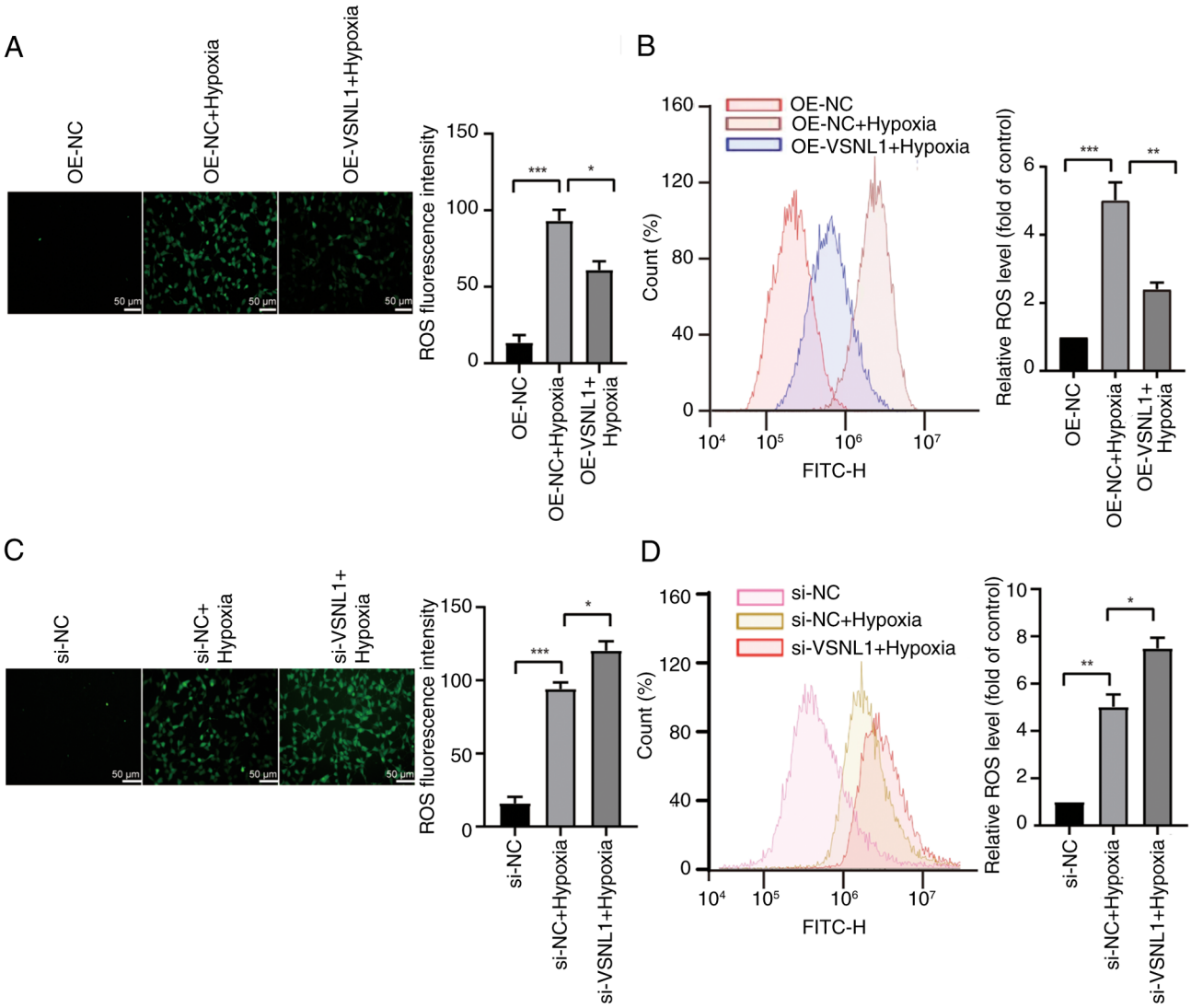

Figure 5. VSNL1 alleviates hypoxia-induced oxidative stress. Representative fluorescence images of ROS in hypoxia-treated AC16 cells following VSNL1 (A) overexpression or (C) knockdown. Scale bar, 50 μm. Quantification of ROS levels in hypoxia-treated AC16 cells assessed by flow cytometry after VSNL1 (B) overexpression or (D) knockdown. *P<0.05, **P<0.01, ***P<0.001. VSNL1, visinin-like protein 1; ROS, reactive oxygen species; OE-NC, overexpression negative control; OE-VSNL1, VSNL1 overexpression; siRNA, small interfering RNA; si-NC, siRNA negative control; si-VSNL1, VSNL1 knockdown via siRNA.

BCL-2 levels and increased BAX protein levels, suggesting that VSNL1 inhibits apoptosis activation and exerts protective effects on cardiomyocytes (Fig. 4H).

To further evaluate whether VSNL1 modulates cardiomyocyte injury related to apoptosis, intracellular levels of MDA, CK-MB and LDH were measured. The results revealed that VSNL1 overexpression markedly reduced the release of these markers (Fig. 4D-F), whereas VSNL1 silencing exacerbated hypoxia-induced cardiomyocyte damage, demonstrated by markedly elevated levels of MDA, CK-MB and LDH (Fig. 4I-K).

VSNL1 alleviates hypoxia-induced oxidative stress during the early phase of myocardial apoptosis. Hypoxia-induced cellular damage is closely associated with elevated ROS levels, a hallmark of oxidative stress (18). ROS serve as key mediators of mitochondria-mediated apoptosis (19,20), characterized by excessive ROS production and loss of MMP (21). To evaluate the role of VSNL1 in alleviating intracellular oxidative stress, ROS accumulation was quantified and visualized using fluorescence microscopy and flow cytometry. The results revealed that the hypoxia-treated cells exhibited a significant increase in green fluorescence intensity (Fig. 5A and B), indicative of excessive ROS accumulation. Notably, overexpression of VSNL1 markedly reduced ROS levels compared with those in the hypoxia group. Conversely, silencing of VSNL1 using siRNA exacerbated oxidative stress, as demonstrated by the increase in ROS levels (Fig. 5C and D). These findings highlighted the role of VSNL1 in alleviating hypoxia-induced oxidative stress during the early phase of myocardial apoptosis.

VSNL1 preserves the MMP in hypoxia-induced myocardial apoptosis. The loss of MMP is a pivotal event that increases mitochondrial outer membrane permeability, representing an early step in the intrinsic apoptotic pathway (22). To evaluate whether VSNL1 influences mitochondrial depolarization, the MMP was measured using JC-1 dye, which detects changes

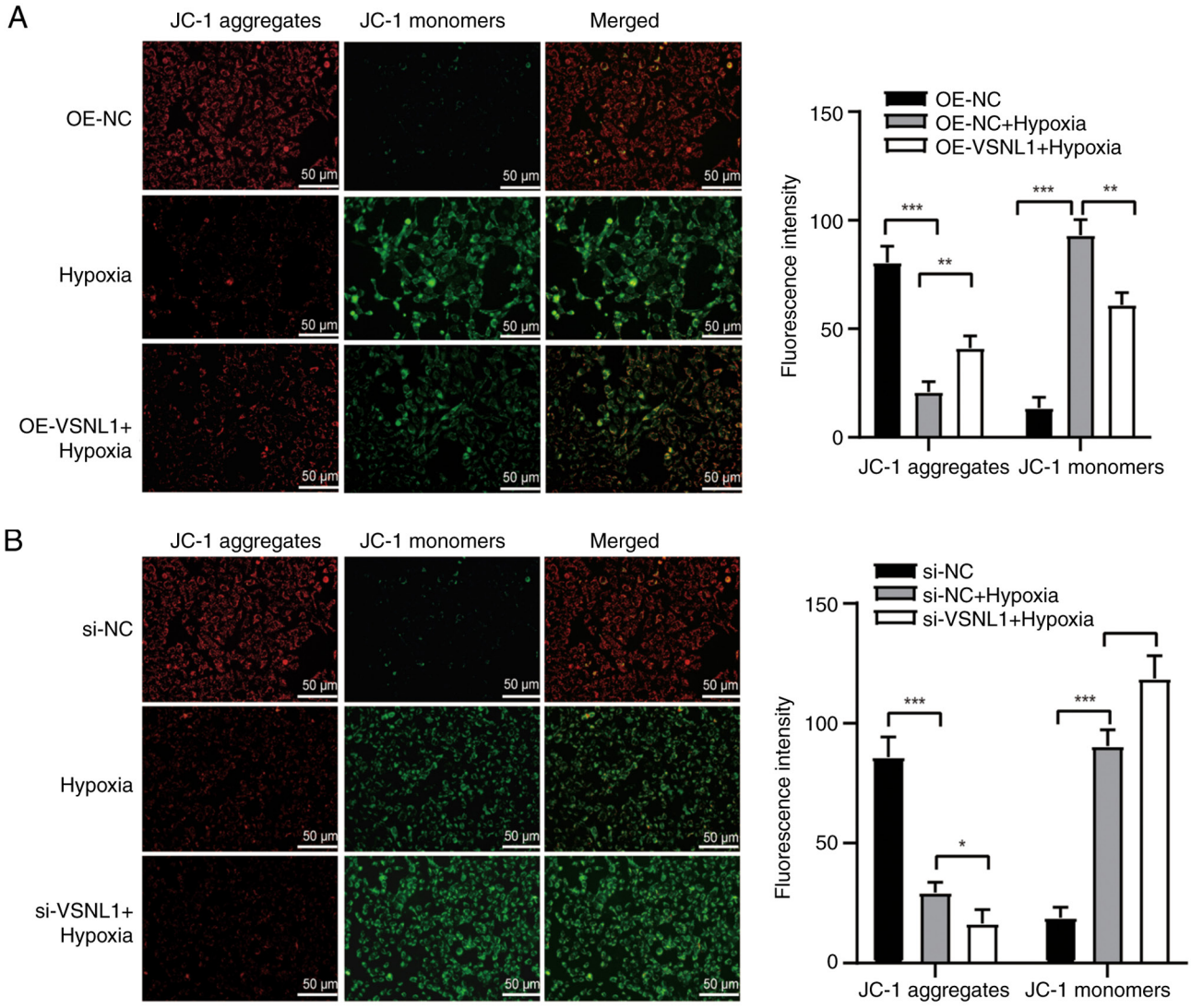

Figure 6. VSNL1 mitigates hypoxia-induced loss of the MMP. Representative fluorescence images of MMP staining in hypoxia-treated AC16 cells following VSNL1 (A) overexpression or (B) knockdown, along with quantification of JC-1 aggregates (red fluorescence) and JC-1 monomers (green fluorescence). Scale bar, 50 μm. *P<0.05; **P<0.01; ***P<0.001. VSNL1, visinin-like protein 1; MMP, mitochondrial membrane potential; OE-NC, overexpression negative control; OE-VSNL1, VSNL1 overexpression; siRNA, small interfering RNA; si-NC, siRNA negative control; si-VSNL1, VSNL1 knockdown via siRNA.

in the MMP via fluorescence shifts. Under hypoxic conditions, a marked increase in JC-1 monomers emitting green fluorescence was observed, along with a near absence of JC-1 aggregates emitting red fluorescence, indicating a substantial loss of MMP. Overexpression of VSNL1 markedly mitigated this effect, reducing green fluorescence and partially restoring red fluorescence, suggesting that VSNL1 overexpression alleviated the loss of MMP (Fig. 6A). By contrast, cells treated with si-VSNL1 under hypoxic conditions exhibited decreased red fluorescence and increased green fluorescence compared with the hypoxia-only group, confirming a pronounced reduction in MMP (Fig. 6B). These findings underscored the essential role of VSNL1 in maintaining the MMP and mitochondrial function, as well as its regulatory effect in attenuating hypoxia-induced myocardial apoptosis.

Mechanistic study of VSNL1-mediated regulation of the CNP/NPRB signaling pathway. To assess the expression changes of the CNP/NPRB signaling pathway during the acute phase of AMI, the present study employed a mouse model of AMI and performed western blot analysis of myocardial tissues from the Sham and AMI groups (24 h post-AMI). The results revealed significant downregulation of CNP protein expression in the AMI group compared with the Sham group. In addition, the expression levels of NPRB were significantly reduced in the AMI group (Fig. 7A). This suggests that suppression of the CNP/NPRB pathway may serve a critical role in the early pathological process of AMI.

To further evaluate the dynamic changes of this signaling pathway under ischemic conditions, an *in vitro* AMI model was established using AC16 cardiomyocytes. Cells were harvested at multiple time points and qPCR analysis was performed. The results demonstrated a continuous decline in mRNA expression levels of both CNP and NPRB over time. Notably, their expression levels at 24 h post-simulation were markedly reduced compared with those at 0 h, supporting the sustained inhibition of the CNP/NPRB pathway during myocardial ischemia (Fig. 7B).

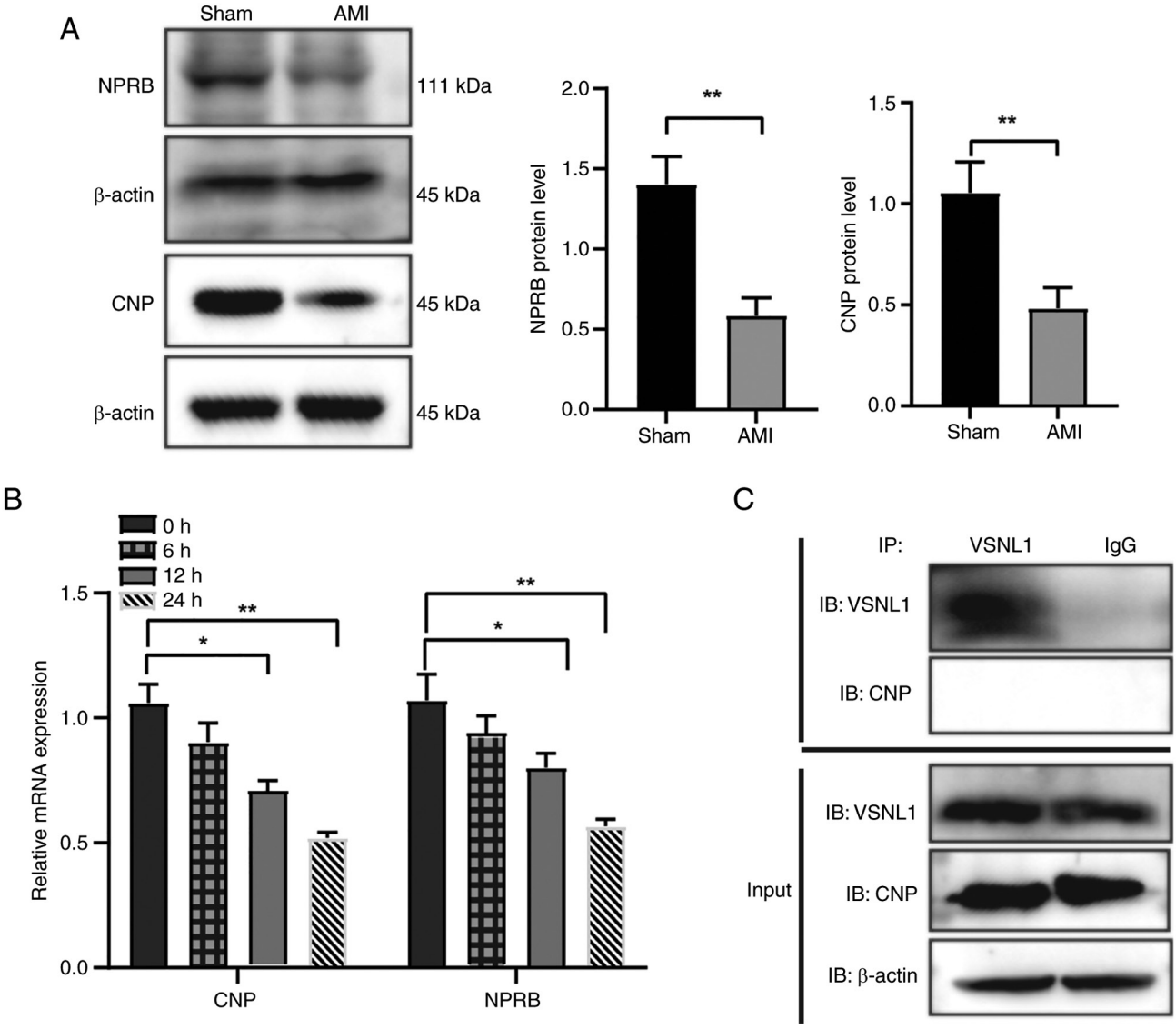

Figure 7. Mechanistic analysis of VSNL1 involvement in the regulation of the CNP/NPRB signaling pathway. (A) Protein expression levels of CNP and NPRB in myocardial tissue following AMI. (B) Time-dependent changes in CNP and NPRB mRNA expression in AC16 cardiomyocytes under ischemic conditions. (C) Co-immunoprecipitation analysis of the interaction between VSNL1 and CNP in AC16 cells. *P<0.05, **P<0.01. VSNL1, visinin-like protein 1; CNP, 2',3'-cyclic nucleotide 3' phosphodiesterase; NPRB, natriuretic peptide receptor B; AMI, acute myocardial infarction; IP, immunoprecipitation; IB, immunoblotting.

To determine whether VSNL1 regulates this pathway via direct protein-protein interaction, a Co-IP assay was performed in AC16 cells. Experimental groups included the VSNL1-IP group, IgG control group and total protein (Input) group. Immunoblotting was performed using anti-VSNL1 and anti-CNP antibodies, and the results revealed that both VSNL1 and CNP proteins were markedly expressed in the Input group, indicating sufficient protein extraction. In the VSNL1-IP group, VSNL1 was successfully precipitated using the anti-VSNL1 antibodies, confirming the validity of the Co-IP system. By contrast, no CNP band was detected in the VSNL1 immunoprecipitated complex, indicating that VSNL1 does not form a stable, direct protein-protein complex with CNP under the experimental conditions used. Additionally, no specific bands were observed in the IgG control group, excluding the possibility of nonspecific binding (Fig. 7C).

In summary, although VSNL1 may participate in cardioprotective processes by modulating the CNP/NPRB signaling pathway, its regulatory mechanism is more likely to be mediated through signaling modulation rather than direct physical interaction.

VSNL1 mediates hypoxia-induced cardiomyocyte apoptosis via the CNP/NPRB pathway. The CNP/NPRB signaling pathway is known for its protective anti-inflammatory and anti-apoptotic effects, particularly in cardiac ischemia-reperfusion injury (23,24). To assess whether VSNL1 regulates apoptosis through this pathway, the present study evaluated its effect on CNP and NPRB expression. The results demonstrated that hypoxia markedly downregulated CNP and NPRB mRNA and protein levels, whereas VSNL1 overexpression restored their expression (Fig. 8A and B). Conversely, VSNL1 knockdown exacerbated their downregulation (Fig. 8C).

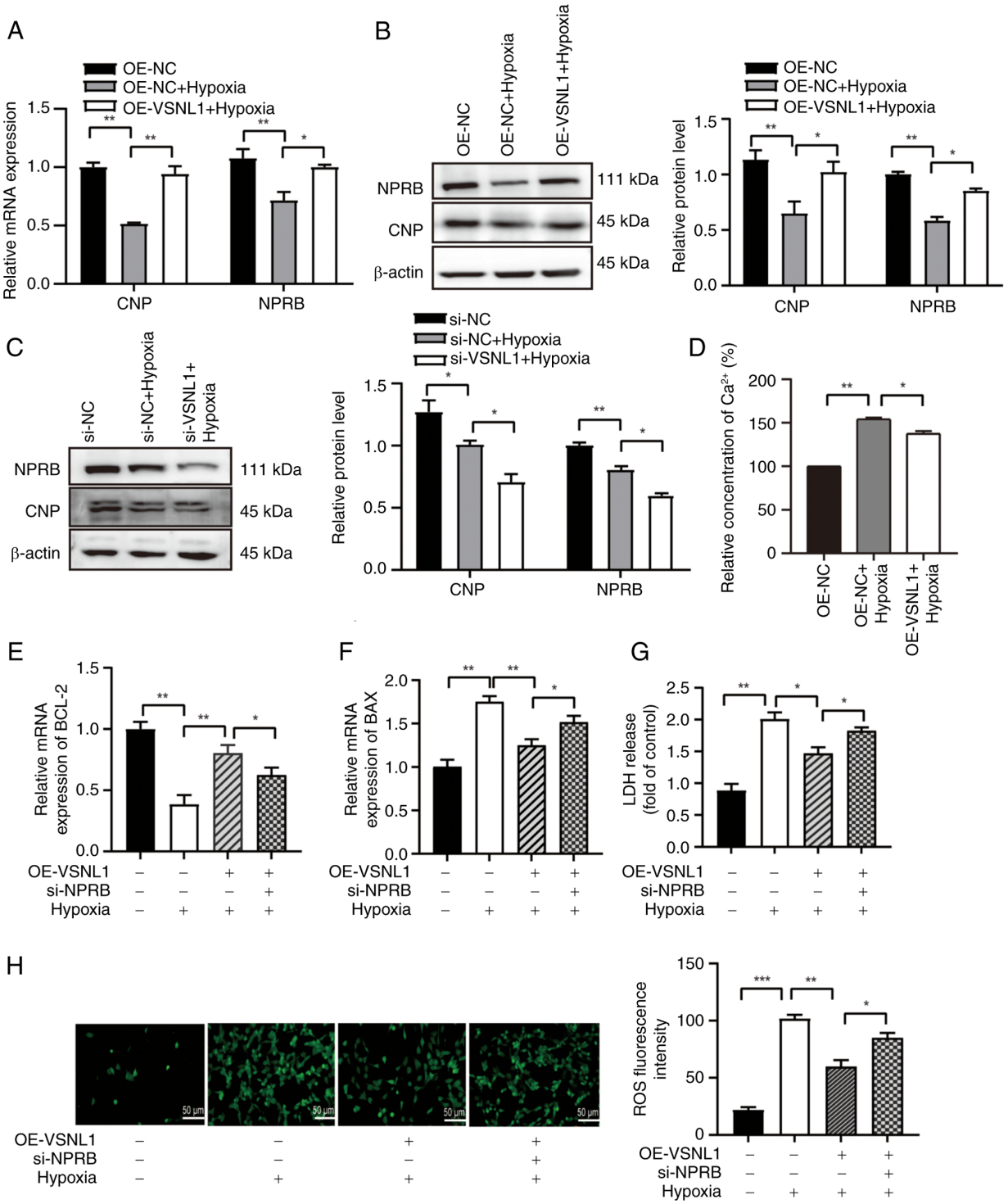

Figure 8. VSNL1 regulates hypoxia-induced apoptosis via the CNP/NPRB pathway in cardiomyocytes. (A) CNP and NPRB expression in hypoxia-exposed AC16 cardiomyocytes following 24 h of VSNL1 overexpression, assessed by qPCR. (B) Protein expression levels of CNP and NPRB in hypoxia-exposed cells and control cells with VSNL1 overexpression, analyzed by western blotting. (C) Protein expression levels of CNP and NPRB following VSNL1 knockdown in hypoxic cells, measured by western blotting. (D) Intracellular Ca^{2+} levels in hypoxia-injured and control cells, with or without VSNL1 overexpression measured after 24 h. (E) BCL-2 and (F) BAX mRNA expression following si-NPRB knockdown and OE-VSNL1 treatment in hypoxia-induced AC16 cardiomyocytes, assessed by qPCR. (G) LDH release was measured in treated AC16 cardiomyocytes, where the treatment consisted of VSNL1 overexpression, NPRB silencing and hypoxic exposure. (H) ROS levels were measured. Scale bar, 50 μm. *P<0.05; **P<0.01; ***P<0.001. VSNL1, visinin-like protein 1; CNP, 2',3'-cyclic nucleotide 3' phosphodiesterase; NPRB, natriuretic peptide receptor B; qPCR, quantitative PCR; OE-NC, overexpression negative control; OE-VSNL1, VSNL1 overexpression; siRNA, small interfering RNA; si-NC, siRNA negative control; si-VSNL1, VSNL1 knockdown via siRNA; si-NPRB, NPRB knockdown via siRNA; LDH, lactate dehydrogenase; ROS, reactive oxygen species.

Hypoxia-induced Ca^{2+} overload is closely associated with cardiomyocyte damage and dysfunction (25). Given the role of VSNL1 in calcium signaling, it was hypothesized that it maintains calcium homeostasis via the CNP/NPRB pathway, which regulates cGMP levels and calcium dynamics critical for myocardial function (26). Supporting this, the findings of

the present study demonstrated that VSNL1 overexpression markedly reduced intracellular Ca^{2+} levels in hypoxia-exposed AC16 cells (Fig. 8D).

To further evaluate the role of the CNP/NPRB pathway in the VSNL1-mediated anti-apoptotic mechanism, NPRB was silenced in VSNL1-overexpressing AC16 cells under hypoxic conditions. The results revealed that NPRB knockdown markedly interrupted the anti-apoptotic effect of VSNL1 by decreasing BCL-2 expression while increasing BAX expression (Fig. 8E and F). Furthermore, NPRB silencing exacerbated cell injury compared with VSNL1 overexpression alone, as indicated by increased LDH release and elevated ROS levels (Fig. 8G and H). To confirm the efficiency of si-NPRB transfection, western blot analysis was performed in cells transfected with si-NPRB alone (without other treatments), and successful knockdown of NPRB was confirmed (Fig. S1). Taken together, these findings highlighted the critical role of CNP/NPRB as a downstream effector of VSNL1 in mitigating hypoxia-induced cardiomyocyte apoptosis.

Discussion

The present study revealed downregulation of VSNL1 in both hypoxia-treated AC16 cardiomyocytes and myocardial tissue from an AMI mouse model, suggesting its potential role in ischemia-induced cardiac injury. Overexpression of VSNL1 effectively mitigated hypoxia-induced cardiomyocyte apoptosis and alleviated associated cellular injury. Mechanically, VSNL1 decreased excessive ROS production and preserved the MMP in the early stages of apoptosis, through the regulation of CNP/NPRB signaling. The protective effect of VSNL1 on cardiomyocyte apoptosis was further demonstrated by silencing of VSNL1, which exacerbated apoptosis. The results further demonstrated that VSNL1 attenuated hypoxia-induced cardiomyocyte apoptosis and elucidated the relevant signaling pathways. These findings provided compelling evidence that VSNL1 protects cardiomyocytes from hypoxia-induced apoptosis by modulating the CNP/NPRB signaling pathway (Fig. 9).

Consistent with previous findings that hypoxia induces apoptosis in cardiomyocytes (27,28), the data from the present study demonstrated that hypoxia triggered apoptosis in AC16 cells. Emerging evidence highlights the role of VSNL1 in cardiac development (29), an area of growing interest in cardiology research. During early embryonic development, VSNL1 is predominantly expressed in the crescent-shaped heart region and, as development progresses, its expression shifts to become more concentrated in the atrial precursors, the venous system and the vascular plexus surrounding pulmonary structures (10). This dynamic expression pattern suggests that VSNL1 serves an important regulatory role in heart formation and structural establishment. In pathological contexts, downregulation of VSNL1 has been observed in myocardial infarction, potentially linked to oxidative stress or ischemic remodeling. However, its specific molecular and cellular roles in the heart remain incompletely understood (30). Aligning with these findings, the present study demonstrated a time-dependent decrease in VSNL1 expression in hypoxia-treated AC16 cardiomyocytes. Furthermore, VSNL1 knockdown markedly exacerbated apoptosis under hypoxic conditions, whereas its overexpression alleviated these effects. These results underscore the pivotal role of VSNL1 in protecting cardiomyocytes from hypoxic injury by regulating apoptosis.

CNP, a key member of the natriuretic peptide family, regulates cardiovascular functions primarily by stimulating cGMP production through its receptor NPRB (31). Despite its low expression levels in the heart, CNP exerts notable paracrine effects on vascular tone, blood pressure, inflammation, angiogenesis and cardiomyocyte function (32-34). Through the NPRB signaling pathway, CNP provides cardioprotection by enhancing contractility, reducing fibrosis and stabilizing cardiac electrophysiology (35-37). Notably, CNP expression is markedly reduced in failing ventricles, with its levels associated with disease severity and prognosis in conditions such as ischemic and dilated cardiomyopathies (38). However, the precise mechanisms through which the CNP/NPRB pathway regulates cardiomyocyte apoptosis and maintains calcium homeostasis in HF remain poorly understood. In the present study, it was demonstrated that hypoxic conditions markedly reduced the expression levels of both CNP and NPRB in AC16 cardiomyocytes. Notably, VSNL1 overexpression activated the CNP/NPRB signaling pathway, whereas VSNL1 knockdown inhibited this pathway. Additionally, siRNA-mediated knockdown of NPRB demonstrated that the reduction of NPRB expression partially compromised the anti-apoptotic effects of VSNL1 overexpression, providing novel insights into the role of the CNP/NPRB signaling pathway in regulating apoptosis in cardiomyocytes.

In HF, dysregulation of Ca^{2+} leads to abnormal myocardial contraction and diastole, disrupting cardiac function (39). CNP negatively regulates protein kinase A and calcium/calmodulin-dependent protein kinase II activity through activation of the cGMP signaling pathway, while affecting Ca^{2+} transient amplitude, demonstrating a complex Ca^{2+} processing regulation (38). Furthermore, knockdown of the calcium-sensing protein VSNL1 has been previously reported to downregulate key calcium-handling proteins [such as sarcoplasmic/endoplasmic reticulum calcium ATPase 2 (SERCA2) and ryanodine receptor 2 (RyR2)] and voltage-dependent Ca^{2+} channels, indicating that VSNL1 may modulate myocardial Ca^{2+} homeostasis, possibly in synergy with the CNP/NPRB pathway (40). The present study demonstrated that hypoxic injury resulted in increased calcium ion levels, whereas overexpression of VSNL1 alleviated hypoxia-induced calcium overload. Therefore, it was hypothesized that calcium ions serve as downstream effectors of the CNP/NPRB pathway, potentially mediated by cGMP-dependent regulation of calcium-handling proteins, which warrants further investigation.

Although the present study did not directly assess the downstream effectors of the CNP/NPRB signaling axis, accumulating evidence strongly supports the existence of a canonical CNP/NPRB/cGMP/protein kinase G (PKG) cascade mediating cardioprotective effects through regulation of oxidative stress, calcium homeostasis and mitochondrial integrity (41-44). Upon activation by CNP, NPRB stimulates membrane-bound guanylyl cyclase activity, elevating intracellular cGMP levels, which in turn activate PKG, which is a key serine/threonine kinase involved in cardiomyocyte survival (41). PKG exerts anti-apoptotic effects by inhibiting mitochondrial permeability transition pore opening through phosphorylation of targets such as cyclophilin D and voltage dependent anion channel

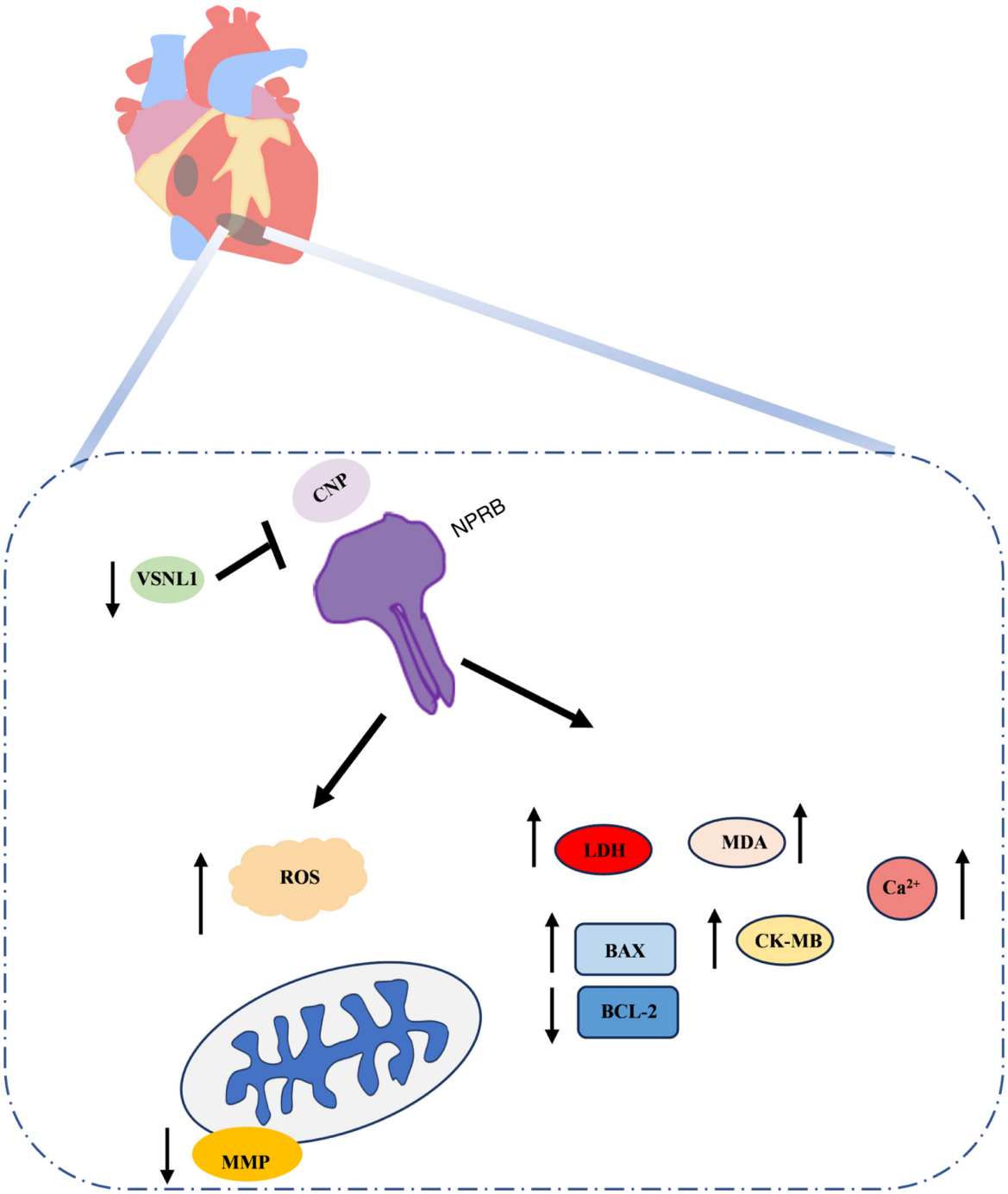

Figure 9. Role of VSNL1 in hypoxic apoptosis and downstream mechanisms. VSNL1, visinin-like protein 1; CNP, 2',3'-cyclic nucleotide 3' phosphodiesterase; NPRB, natriuretic peptide receptor B; MMP, mitochondrial membrane potential; ROS, reactive oxygen species; LDH, lactate dehydrogenase; MDA, malonaldehyde; CK-MB, creatine kinase-MB.

1, thereby preserving mitochondrial function and suppressing cytochrome *c*-mediated apoptosis (42).

PKG serves a critical role in calcium handling by enhancing SERCA2a activity, inhibiting phospholamban and RyR2 function, and modulating Na^+/Ca^{2+} exchanger activity. These actions collectively promote efficient sarcoplasmic reticulum Ca^{2+} reuptake, prevent cytosolic calcium overload and maintain contractility under pathological conditions such as ischemia-reperfusion injury (43,44).

While the current study primarily focused on the upstream regulation and anti-apoptotic effects of VSNL1 via the CNP/NPRB axis, elucidating the downstream signaling events is essential to comprehensively understand the mechanism. As a future research direction, it is intended to investigate the activation status of PKG and the expression or modulation of calcium-handling proteins in response to VSNL1 regulation, using both molecular and functional assays. These future studies will aim to clarify whether the CNP/NPRB-mediated cardioprotection involves cGMP signaling and calcium homeostasis pathways.

In the present study, overexpression of VSNL1 resulted in reduced ROS accumulation, stabilization of the MMP and

attenuation of calcium dysregulation, which are phenotypes that closely mirror the known downstream effects of PKG activation. As VSNL1 is a neuronal calcium sensor protein with EF-hand motifs and high calcium affinity (45), it is plausible that VSNL1 synergizes with the CNP/NPRB/cGMP/PKG signaling axis to fine-tune calcium flux and mitochondrial function, particularly within specialized microdomains such as the sarcoplasmic reticulum-mitochondria interface.

It can be hypothesized that VSNL1 enhances the cardioprotective effects of CNP/NPRB signaling through the following pathways: i) Facilitating intracellular calcium buffering to mitigate calcium overload; ii) interacting with calcium-handling proteins to stabilize their expression or phosphorylation; and iii) serving as a scaffolding protein that spatially couples PKG with its downstream effectors. While direct biochemical validation remains necessary, the current literature provides a robust theoretical framework supporting the involvement of the cGMP/PKG axis in mediating the cardioprotective effects observed with VSNL1 overexpression (13,46). These insights establish a plausible mechanistic link between VSNL1 and natriuretic peptide signaling and highlight VSNL1 as a potential therapeutic node for ischemic heart disease.

In conclusion, the present study highlighted the role of VSNL1 in alleviating hypoxia-induced cardiomyocyte apoptosis and the potential for developing novel therapeutic strategies, such as VSNL1 agonists, offering promising clinical implications. Nonetheless, an important limitation should be noted: While the AC16 cell line is of human origin, its phenotype differs from that of mature cardiomyocytes. To strengthen the reliability and clinical relevance of the findings of the present study, future research should validate these results using experimental animal models that more closely replicate the physiological conditions of the human heart, as well as primary cardiomyocytes. Such approaches will provide stronger evidence for translating these insights into therapeutic strategies.

Acknowledgements

Not applicable.

Funding

The present study was funded by the Shanghai Science and Technology Innovation Action Plan (grant nos. 21S11901700 and 22010502600), the Shanghai Natural Science Foundation (grant no. 21ZR1428400) and the Clinical Research Project of Pudong New Area Health Commission (Grant No. 2025-PWYC-14), Shanghai, China.

Availability of data and materials

The data generated in the present study may be requested from the corresponding author.

Authors' contributions

YL and XC were responsible for the conceptualization and design of the study. Material preparation, data collection and analysis were performed by XY, WF, RC and LM. The manuscript was drafted by XY, XC and YL, who also critically revised it for important intellectual content. YL and XC confirm the authenticity of all the raw data. All authors have read and approved the final manuscript.

Ethics approval and consent to participate

All animal experimental procedures in the present study were reviewed and approved by the Ethics Committee of Shanghai University of Medicine and Health Sciences (approval no. 2021-SZR-05-410482198512239314; Shanghai, China).

Patient consent for publication

Not applicable.

Competing interests

The authors declare that they have no competing interests.

References

1. Yu X, Yang Y, Chen T, Wang Y, Guo T, Liu Y, Li H and Yang L: Cell death regulation in myocardial toxicity induced by antineoplastic drugs. Front Cell Dev Biol 11: 1075917, 2023.
2. Chen XJ, Liu SY, Li SM, Feng JK, Hu Y, Cheng XZ, Hou CZ, Xu Y, Hu M, Feng L and Xiao L: The recent advance and prospect of natural source compounds for the treatment of heart failure. Heliyon 10: e27110, 2024.
3. Jiang M, Fan X, Wang Y and Sun X: Effects of hypoxia in cardiac metabolic remodeling and heart failure. Exp Cell Res 432: 113763, 2023.
4. Chen Z, Zhang S, Guo C, Li J and Sang W: Downregulation of miR-200c protects cardiomyocytes from hypoxia-induced apoptosis by targeting GATA-4. Int J Mol Med 39: 1589-1596, 2017.
5. Zhang X, Hu C, Kong CY, Song P, Wu HM, Xu SC, Yuan YP, Deng W, Ma ZG and Tang QZ: FNDC5 alleviates oxidative stress and cardiomyocyte apoptosis in doxorubicin-induced cardiotoxicity via activating AKT. Cell Death Differ 27: 540-555, 2020.
6. Ma L, Liu M, Liu C, Zhang H, Yang S, An J, Qu G, Song S and Cao Q: Research progress on the mechanism of the antitumor effects of cannabidiol. Molecules 29: 1943, 2024.
7. Li C, Liu X, Li J, Lai J, Su J, Zhu B, Gao B, Li Y and Zhao M: Selenomethionine inhibited HADV-induced apoptosis mediated by ROS through the JAK-STAT3 signaling pathway. Nutrients 16: 1966, 2024.
8. Hao M, Liu Y, Chen P, Jiang H and Kuang HY: Astragaloside IV protects RGC-5 cells against oxidative stress. Neural Regen Res 13: 1081-1086, 2018.
9. Tage H, Yamaguchi K, Nakagawa S, Kasuga S, Takane K, Furukawa Y and Ikenoue T: Visinin-like 1, a novel target gene of the Wnt/β-catenin signaling pathway, is involved in apoptosis resistance in colorectal cancer. Cancer Med 12: 13426-13437, 2023.
10. Ola R, Lefebvre S, Braunewell KH, Sainio K and Sariola H: The expression of Visinin-like 1 during mouse embryonic development. Gene Expr Patterns 12: 53-62, 2012.
11. He C, Liu W, Xiong Y, Wang Y, Pan L, Luo L, Tu Y, Song R and Chen W: VSNL1 promotes cell proliferation, migration, and invasion in colorectal cancer by binding with COL10A1. Ann Clin Lab Sci 52: 60-72, 2022.
12. Aiba T, Hijiya N, Akagi T, Tsukamoto Y, Hirashita Y, Kinoshita K, Uchida T, Nakada C, Kurogi S, Ueda Y, *et al*: Overexpression of VSNL1 enhances cell proliferation in colorectal carcinogenesis. Pathobiology 91: 121-131, 2024.
13. Braunewell KH, Brackmann M, Schaupp M, Spilker C, Anand R and Gundelfinger ED: Intracellular neuronal calcium sensor (NCS) protein VILIP-1 modulates cGMP signalling pathways in transfected neural cells and cerebellar granule neurones. J Neurochem 78: 1277-1286, 2001.
14. Williams TA, Monticone S, Crudo V, Warth R, Veglio F and Mulatero P: Visinin-like 1 is upregulated in aldosterone-producing adenomas with KCNJ5 mutations and protects from calcium-induced apoptosis. Hypertension 59: 833-839, 2012.

15. Tan BL, Norhaizan ME and Chan LC: *Manilkara Zapota* (L.) P. Royen leaf water extract induces apoptosis in human hepatocellular carcinoma (HepG2) Cells via ERK1/2/Akt1/JNK1 signaling pathways. Evid Based Complement Alternat Med 2018: 7826576, 2018.
16. Livak KJ and Schmittgen TD: Analysis of relative gene expression data using real-time quantitative PCR and the 2(-Delta Delta C(T)) method. Methods 25: 402-408, 2001.
17. Chang X, Zhang T, Wang J, Liu Y, Yan P, Meng Q, Yin Y and Wang S: SIRT5-related desuccinylation modification contributes to quercetin-induced protection against heart failure and high-glucose-prompted cardiomyocytes injured through regulation of mitochondrial quality surveillance. Oxid Med Cell Longev 2021: 5876841, 2021.
18. Peng J, Yang Z, Li H, Hao B, Cui D, Shang R, Lv Y, Liu Y, Pu W, Zhang H, *et al*: Quercetin reprograms immunometabolism of macrophages via the SIRT1/PGC-1α signaling pathway to ameliorate lipopolysaccharide-induced oxidative damage. Int J Mol Sci 24: 5542, 2023.
19. Zhang Y, Chen G, Zhuang X and Guo M: Inhibition of growth of colon tumors and proliferation of HT-29 cells by *Warburgia ugandensis* extract through mediating G_0/G_1 cell cycle arrest, cell apoptosis, and intracellular ROS generation. Oxid Med Cell Longev 2021: 8807676, 2021.
20. Owari T, Tanaka N, Nakai Y, Miyake M, Anai S, Kishi S, Mori S, Fujiwara-Tani R, Hojo Y, Mori T, *et al*: 5-Aminolevulinic acid overcomes hypoxia-induced radiation resistance by enhancing mitochondrial reactive oxygen species production in prostate cancer cells. Br J Cancer 127: 350-363, 2022.
21. Deng F, Wang S, Cai S, Hu Z, Xu R, Wang J, Feng D and Zhang L: Inhibition of caveolae contributes to propofol preconditioning-suppressed microvesicles release and cell injury by hypoxia-reoxygenation. Oxid Med Cell Longev 2017: 3542149, 2017.
22. Ma J, Yu W, Wang Y, Cao G, Cai S, Chen X, Yan N, Yuan Y, Zeng H, Fleenor DL, *et al*: Neuroprotective effects of C-type natriuretic peptide on rat retinal ganglion cells. Invest Ophthalmol Vis Sci 51: 3544-3553, 2010.
23. Jin X, Zhang Y, Li X, Zhang J and Xu D: C-type natriuretic peptide ameliorates ischemia/reperfusion-induced acute kidney injury by inhibiting apoptosis and oxidative stress in rats. Life Sci 117: 40-45, 2014.
24. Ruhr IM, Shiels HA, Crossley DA II and Galli GLJ: Developmental programming of sarcoplasmic reticulum function improves cardiac anoxia tolerance in turtles. J Exp Biol 227: jeb247434, 2024.
25. Abuzaanona A and Lanfear D: Pharmacogenomics of the natriuretic peptide system in heart failure. Curr Heart Fail Rep 14: 536-542, 2017.
26. Hu D, Gu Y, Wu D, Zhang J, Li Q, Luo J, Li S, Yuan Z and Zhu B: Icariside II protects cardiomyocytes from hypoxia-induced injury by upregulating the miR-7-5p/BTG2 axis and activating the PI3K/Akt signaling pathway. Int J Mol Med 46: 1453-1465, 2020.
27. Xie X, Ji Q, Han X, Zhang L and Li J: Knockdown of long non-coding RNA TTTY15 protects cardiomyocytes from hypoxia-induced injury by regulating let-7b/MAPK6 axis. Int J Clin Exp Pathol 13: 1951-1961, 2020.
28. Fan W, Yang C, Hou X, Wan J and Liao B: Novel insights into the sinoatrial node in single-cell RNA sequencing: From developmental biology to physiological function. J Cardiovasc Dev Dis 9: 986, 2022.
29. Buttgereit J, Qadri F, Monti J, Langenickel TH, Dietz R, Braunewell KH and Bader M: Visinin-like protein 1 regulates natriuretic peptide receptor B in the heart. Regul Pept 161: 51-57, 2010.
30. Mei C, Kang Y, Zhang C, He C, Liao A and Huang D: C-type natriuretic peptide plays an anti-inflammatory role in rat epididymitis induced by *UPEC*. Front Cell Infect Microbiol 11: 711842, 2021.
31. Nakagawa Y and Nishikimi T: CNP, the third natriuretic peptide: Its biology and significance to the cardiovascular system. Biology (Basel) 11: 986, 2022.
32. Bubb KJ, Aubdool AA, Moyes AJ, Lewis S, Drayton JP, Tang O, Mehta V, Zachary IC, Abraham DJ, Tsui J and Hobbs AJ: Endothelial C-type natriuretic peptide is a critical regulator of angiogenesis and vascular remodeling. Circulation 139: 1612-1628, 2019.
33. Moyes AJ and Hobbs AJ: C-type Natriuretic peptide: A multifaceted paracrine regulator in the heart and vasculature. Int J Mol Sci 20: 2281, 2019.
34. Pernomian L, Prado AF, Silva BR, Azevedo A, Pinheiro LC, Tanus-Santos JE and Bendhack LM: C-type natriuretic peptide induces anti-contractile effect dependent on nitric oxide, oxidative stress, and NPR-B activation in sepsis. Front Physiol 7: 226, 2016.
35. Dorey TW, Liu Y, Jansen HJ, Bohne LJ, Mackasey M, Atkinson L, Prasai S, Belke DD, Fatehi-Hassanabad A, Fedak PWM and Rose RA: Natriuretic peptide receptor B protects against atrial fibrillation by controlling atrial cAMP via phosphodiesterase 2. Circ Arrhythm Electrophysiol 16: e012199, 2023.
36. Dorey TW, Mackasey M, Jansen HJ, McRae MD, Bohne LJ, Liu Y, Belke DD, Atkinson L and Rose RA: Natriuretic peptide receptor B maintains heart rate and sinoatrial node function via cyclic GMP-mediated signalling. Cardiovasc Res 118: 1917-1931, 2022.
37. Cachorro E, Günscht M, Schubert M, Sadek MS, Siegert J, Dutt F, Bauermeister C, Quickert S, Berning H, Nowakowski F, *et al*: CNP promotes antiarrhythmic effects via phosphodiesterase 2. Circ Res 132: 400-414, 2023.
38. Dabravolski SA, Sadykhov NK, Kartuesov AG, Borisov EE, Sukhorukov VN and Orekhov AN: Interplay between Zn^{2+} homeostasis and mitochondrial functions in cardiovascular diseases and heart ageing. Int J Mol Sci 23: 6890, 2022.
39. Liang D, Xue J, Geng L, Zhou L, Lv B, Zeng Q, Xiong K, Zhou H, Xie D, Zhang F, *et al*: Cellular and molecular landscape of mammalian sinoatrial node revealed by single-cell RNA sequencing. Nat Commun 12: 287, 2021.
40. O'Rourke B, Van Eyk JE and Foster DB: Mitochondrial protein phosphorylation as a regulatory modality: Implications for mitochondrial dysfunction in heart failure. Congest Heart Fail 17: 269-282, 2011.
41. Potter LR, Abbey-Hosch S and Dickey DM: Natriuretic peptides, their receptors, and cyclic guanosine monophosphate-dependent signaling functions. Endocr Rev 27: 47-72, 2006.
42. Inserte J and Garcia-Dorado D: The cGMP/PKG pathway as a common mediator of cardioprotection: Translatability and mechanism. Br J Pharmacol 172: 1996-2009, 2015.
43. Takimoto E, Champion HC, Li M, Belardi D, Ren S, Rodriguez ER, Bedja D, Gabrielson KL, Wang Y and Kass DA: Chronic inhibition of cyclic GMP phosphodiesterase 5A prevents and reverses cardiac hypertrophy. Nat Med 11: 214-222, 2005.
44. Zhazykbayeva S, Budde H, Kaçmaz M, Zemedie Y, Osman H, Hassoun R, Jaquet K, Akin I, El-Battrawy I and Herwig M: Exploring PKG signaling as a therapeutic avenue for pressure overload, ischemia, and HFpEF. Expert Opin Ther Targets 28: 857-873, 2024.
45. Dai QQ, Wang YY, Jiang YP, Li L and Wang HJ: VSNL1 promotes gastric cancer cell proliferation and migration by regulating P2X3/P2Y2 receptors and is a clinical indicator of poor prognosis in gastric cancer patients. Gastroenterol Res Pract 2020: 7241942, 2020.
46. Brackmann M, Schuchmann S, Anand R and Braunewell KH: Neuronal Ca2+ sensor protein VILIP-1 affects cGMP signalling of guanylyl cyclase B by regulating clathrin-dependent receptor recycling in hippocampal neurons. J Cell Sci 118: 2495-2505, 2005.